

W0 3695

UCRL-1097

Unclassified - Physics Distribution

- 1 -

UNIVERSITY OF CALIFORNIA

Radiation Laboratory

**UNCLASSIFIED**

PROTON-PROTON SCATTERING AT 105 MEV AND 75 MEV.\*

Robert W. Birge\*\*, Ulrich E. Kruse and Norman F. Ramsey

Harvard University, Cambridge, Massachusetts

January 31, 1951

\*Assisted by the Joint Program of the ONR and the AEC.

\*\*Now at the Radiation Laboratory, University of California, Berkeley

This document is  
**PUBLICLY RELEASABLE**  
Hugh Kinsey  
Authorizing Official  
Date 6/10/08

Berkeley, California

0100  
УПРАВЛЕНИЕ  
МЕСТНОГО САМОУПРАВЛЕНИЯ  
ИМУЩЕСТВА И ПРЕДПРИЯТИЙ  
ИЗДАНИЕ № 1

Содержание

Содержание

Содержание

Содержание

Содержание

Содержание

Содержание

Содержание

Содержание

## **DISCLAIMER**

**This report was prepared as an account of work sponsored by an agency of the United States Government. Neither the United States Government nor any agency Thereof, nor any of their employees, makes any warranty, express or implied, or assumes any legal liability or responsibility for the accuracy, completeness, or usefulness of any information, apparatus, product, or process disclosed, or represents that its use would not infringe privately owned rights. Reference herein to any specific commercial product, process, or service by trade name, trademark, manufacturer, or otherwise does not necessarily constitute or imply its endorsement, recommendation, or favoring by the United States Government or any agency thereof. The views and opinions of authors expressed herein do not necessarily state or reflect those of the United States Government or any agency thereof.**

## **DISCLAIMER**

**Portions of this document may be illegible in electronic image products. Images are produced from the best available original document.**

## PROTON-PROTON SCATTERING AT 105 MEV AND 75 MEV.\*

Robert W. Birge\*\*, Ulrich E. Kruse and Norman F. Ramsey

Harvard University, Cambridge, Massachusetts.

January 31, 1951

I Introduction

The scattering of protons by protons provides an important method for studying the nature of nuclear forces. At low energies, less than five Mev, the deBroglie wavelength  $\lambda$  of a proton is large compared to the range of nuclear forces and the interaction is effective only in states of zero orbital angular momentum (S states). Recent proton-proton scattering experiments at energies as high as thirty Mev<sup>1</sup> have failed to show any appreciable contribution to the cross section from higher angular momentum states, but it is necessary to bring in tensor forces to explain the magnitude of the observed cross section.<sup>2</sup>

Further experiments now in progress at Berkeley,<sup>3</sup> in the 350 Mev

---

\*Assisted by the Joint Program of the ONR and the AEC.

\*\*Now at the Radiation Laboratory, University of California, Berkeley.

<sup>1</sup>W. K. H. Panofsky and F. L. Fillmore, Phys. Rev. 79, 57 (1950) ;

Cork, Johnston, and Richman, Phys. Rev. 79, 71 (1950).

<sup>2</sup>R. S. Christian and H. P. Noyes, Phys. Rev. 79, 85 (1950) ;

H. Yamauchi, Ph.D. Thesis, Harvard, 1950.

<sup>3</sup>O. Chamberlain and C. Wiegand, Phys. Rev. 79, 81 (1950) ;

Chamberlain, Segrè, and Wiegand, Bull. Amer. Phys. Soc. Vol 25 #6, J8 (1950)

region, indicate spherical symmetry, but with twice the cross section that can be explained theoretically by the use of central force scattering theory. Because of these unusual results at high energies, the 100 Mev region is of particular interest.

The experiment described here used the internal beam of 115 Mev protons made available by the operation of the Harvard 95-inch frequency-modulated cyclotron. A brief description of the equipment and some of the results has already appeared<sup>4</sup>, hence the chief purpose of this paper is to give in somewhat more detail the techniques used and problems encountered in the experiment.

## II Description of Equipment.

### A. Target

The internal proton beam is intercepted by a ten-mil polyethylene,  $(CH_2)_n$ , target and the recoil and scattered protons in the vertical plane are detected in coincidence as in the method of Wilson and Creutz<sup>5</sup> and as in the scattering experiments of Oxley<sup>6</sup> which use an internal cyclotron beam. This method effectively eliminates the background due to protons scattered from the carbon in the target. The polyethylene foil is partially melted onto two 0.4 mil tungsten wires that are suspended vertically in a "C" shaped frame attached to a long target probe. The

---

<sup>4</sup>R. W. Birge, Phys. Rev. 80, 490 (1950).

<sup>5</sup>R. R. Wilson and E. C. Creutz, Phys. Rev. 71, 339 (1947).

<sup>6</sup>C. L. Oxley, Phys. Rev. 76, 461 (1949).

foil may then be easily removed and its radioactivity measured in a manner described in section IIIC.

#### B. Counters

The counters used to detect the scattered protons were anthracene scintillation crystals mounted in slots cut in the ends of short pieces of lucite. These pieces were then clamped to seven foot lucite rods that transmitted the light flashes to RCA 5819 photomultiplier tubes placed in magnetic shields. One counter, used to define the solid angle, measured protons scattered at angles from  $15^\circ$  to  $45^\circ$  with respect to the incident beam, while the other, or monitor counter, was much larger and intercepted the recoil protons at angles from  $45^\circ$  to  $75^\circ$ . Figure 1 shows proton paths for the two limits mentioned, while Figure 2 is a top view for one extreme position.

To facilitate the large linear motion necessary for the defining counter, a ball and socket joint was designed, which provides an angular swing of  $60^\circ$ . It is similar to a design reported elsewhere<sup>7</sup>, and is made of a nonmagnetic stainless steel ball set in a brass socket with an "O" ring gasket on the circumference to make the vacuum seal. The monitor probe has a flexible sylphon joint and can be moved through an angle of about  $20^\circ$  in the horizontal plane. Both probes consist of stainless steel tubes acting as both light shields and vacuum containers. The details are shown in Figure 3. In addition to their angular motion the probes may be moved in and out, by sliding them through chevron seals, thus it was possible to perform the experiment with the scatterer at 40

---

<sup>7</sup> O. Retzloff, Rev. Sci. Inst. 20, 324 (1949).

-5-

inches and 35 inches from the center of the cyclotron by suitably moving the three probes radially. The chevron seals are located in a housing behind the large Crane valves, and together with the valves, they constitute a small vacuum lock, which allows removal of the probes without affecting the main cyclotron vacuum system. The small locks speeded up the numerous target changes necessary in the final runs. Because the concrete shielding of the cyclotron is only six feet back from the tank, the probes have a joint part way back, which must be disconnected to remove them from the tank. This joint, like others on the system, employs a standard vacuum technique, namely an "O" ring gasket between two flanges, but it acts as a light-tight joint.

The two probes differ in the following respects. The defining counter probe receives only protons from 40 Mev up and these high energy protons can easily penetrate the wall of the stainless steel tube, which is thinned down to 0.016 inch at the end where the crystal is located. The back end of the probe is bolted down to a rigid table in a position that depends on the angle to be studied. The monitor probe must detect particles with energies as low as eight Mev. To do this a light-tight cap with a one mil aluminum window is used. The cap is placed over the end of the probe and has a baffle at the end to allow the interior to be pumped out, since the aluminum could not withstand the vacuum. The vacuum seal is then made inside the probe, about an inch back, by an "O" ring resting directly on the lucite rod. This arrangement causes some light loss but the amount is not appreciable. The rear end of the probe swivels on a ball bearing mounted on a small bench milling machine, firmly bolted



to the floor. This table can be moved by remote control from the control room of the cyclotron, where selsyn indicators are also located. In this manner the large monitor crystal may be moved inside the tank until the center of a coincidence counting rate plateau is reached.

A great many precautions were taken to insure that as much light as possible could reach the phototubes. Advantage was taken of the fact that when the diameter of the lucite rod increases along the light path, the light rays tend to straighten out. This effect not only cuts down the number of reflections but allows the light to go straight into the phototube rather than to be sprayed out tangent to the end surface. The crystal holders were rounded off around the point where the crystal was set, and were covered with aluminum foil to act as a reflector for light starting out sideways. It was found that merely butting flat ends of lucite together made as good a joint as much more complicated connections. The entire setup when tested on the bench appeared to attenuate the pulses by a factor of about two. A previous setup, which used extruded rather than cast lucite, gave an attenuation factor of ten. Such an attenuation would have made the experiment impossible since lucite itself scintillates very weakly and  $\gamma$ - rays or other radiation, when striking the lucite near the phototube, would have swamped the true signal. A small amount of Canada balsam was used to make optical contact between the crystal and the lucite in the detector probe. In the monitor probe, where the crystal is in the vacuum system, the balsam boiled out. To avoid this difficulty the crystal was fastened with Duco cement and optical contact was made with mineral oil. The Duco cement itself had

-7-

very poor optical properties when dried and hence could be used only around the edges.

With the arrangement described and because the light flashes from high energy protons in anthracene are quite large, it was possible to operate the phototubes at such a level that no appreciable thermal noise was counted. With the amplifiers set at twice the gain normally used, four single channel counts per minute were recorded with the cyclotron running but with no anthracene crystal in place.

#### C. Amplifying and Counting Systems

The pulses from the photomultiplier tubes went directly to cathode followers, each of which fed 250 feet of RG 62/U cable terminated in its characteristic impedance of 95 ohms. The lengths of the two lines were compared by observing reflections of fast pulses on the scope. The difference was found to be less than 0.01  $\mu$  second. This figure was certainly satisfactory since a coincidence resolving time of 0.2  $\mu$  second was used. The pulses were next amplified by means of commercial versions of the Jordan-Bell linear amplifier<sup>8</sup> and were fed from discriminators in the coincidence circuit,<sup>9</sup> and then into a scaler. The scalers and amplifiers were built by the Atomic Instrument Co., Cambridge, Mass.

Amplifiers used with a pulsed beam such as is present in an f-m cyclotron, sharply limit the possible counting rates unless the dead time is a small fraction of the burst time. The individual bursts on the

---

<sup>8</sup> W. H. Jordan and P. R. Bell, Rev. Sci. Inst. 18, 703 (1947).

<sup>9</sup> Howland, Schröder, and Shipman, Jr., Rev. Sci. Inst. 18, 551 (1947).

Harvard cyclotron lasted about 250  $\mu$  seconds and hence the amplifiers were modified to cut the dead time to about 1  $\mu$  second, and further changes cut the rise time to about 0.1  $\mu$  second.<sup>10</sup> Crystal diodes were inserted within one of the feedback loops to prevent double pulsing when the amplifiers were overloaded.<sup>11</sup>

#### D. Solid Angles

The scattered protons leaving the target travel on helices to reach the counters. The radius of any given helix depends for two reasons on the angle that the particle trajectory makes with the horizontal plane. First, the momentum of the particle depends on the scattering angle and second, only the component of momentum perpendicular to the magnetic field is effected by the field. When the particles scattered in the vertical plane reach the top or bottom of the magnet gap they will have moved inward radially from the incident proton orbit because of their smaller momentum and angle with respect to the field. It turns out that the distance they have gone in is very small (about 1/4 inch out of 40 inches original radius) and very nearly constant for all scattering angles. For all positions studied it was also necessary to calculate the angle in the horizontal plane at which the protons strike the probe, in order that the crystals could be set perpendicular to the scattered proton direction. A first approximation to the solid angle of the defining counter is then just the crystal area divided by the square of the distance traversed. Because of the focussing action of the magnetic field,

---

<sup>10</sup> D. Bodansky, Ph.D. Thesis, Harvard, 1950.

<sup>11</sup> W. G. Cross, Phys. Rev. 78, 185 (1950).

a small correction amounting to a few percent must be made to the solid angle thus calculated. The correction is just  $\sin \psi / \psi$  where  $\psi$  is the angular distance that the proton travels around the helix.

### III Experimental Procedures and Equipment Performance.

#### A. Alignment of Apparatus

With the cyclotron running, curves were plotted of the coincidence rate versus monitor position normalized to the singles rate in the defining counter. A plateau is obtained in these curves, as is shown in Figure 4 if the monitor crystal is sufficiently large. The percent coincidence counts to single channel counts for four minute runs are plotted. Accidental counts have been subtracted out for each point. The counting rate at the top of the plateau was three counts per second for coincidences, about fifteen counts per second in the defining counter and 150 counts per second in the monitor. With a repetition rate of 100 per second, these figures imply one to two monitor counts per burst.

After the counters were set in the correct positions as determined by the coincidence plateaus, it was necessary to rotate the defining crystal about the axis of that probe, to check for misalignment. This procedure was especially necessary if the crystals were long and thin since the side of the crystal rapidly presented a very large area to the beam, with only a small rotation. Plotting coincidences against rotation, now normalized to the monitor single channel rate, one found a minimum and this was the correct position. When the crystal was very short, as

-10-

in the final runs, the rate did not rise rapidly with rotation and the minimum was shallow and broad.

One further check of the apparatus consisted of taking curves of coincidence rate versus amplifier gain. One obtained flat gain curves down to a point where they cut off sharply. This result is not unexpected since the cathode follower limited the pulse heights. However, to really check the pulse height distribution, the following experiment was performed. A thin, 1/8-inch monitor crystal was built and run at a position such that seventy Mev protons would reach it. The counted coincidence protons penetrated the crystal squarely, losing about five Mev since the monitor was set in the middle of a plateau. Then the voltage on the phototube was lowered until the cathode follower was no longer limiting the pulse height. In this manner the curve shown in Figure 5 was obtained. The differential pulse height distribution taken from these data has a width of about 25 percent, which was considered satisfactory in view of the complicated optical system. It was necessary to run gain curves for both the monitor and defining crystals at each angle studied since the particles lost different amounts of energy in the crystal at each position.

#### B. Background and Accidental Coincidences.

In any double coincidence setup there are bound to be accidental coincidences due to the finite resolving time of the coincidence circuit. In the setup used, most of the single channel rate consisted of protons scattered from the carbon in the target. When the counters are moved out of line, no true coincidences should be counted and the remaining rate

-11-

must be due to accidental coincidences. On the other hand, when one channel is delayed with respect to the other, a measure of the accidental coincidence rate is also obtained, since the particles arrive randomly in time. This statement is true, of course, only if the delay time,  $2 \mu$  seconds, is short compared to the burst time,  $250 \mu$  seconds, and if the resolving time,  $0.2 \mu$  second, is large compared to the time of revolution of the particles,  $0.05 \mu$  second. An oscilloscope was used to detect any possible fine structure in the beam that might cause dead spots to appear two  $\mu$  seconds after any given pulse. There appeared to be as many pulses in that region as anywhere else in the burst. With the counting rates used, accidental coincidences usually amounted to only one percent of the true coincidences but occasionally the accidental rate was as high as ten percent. It is preferable to use a delayed coincidence rate as a measure of accidentals rather than to count a background later with the counters out of line. The reason is that accidentals are proportional to the square of the beam intensity for double coincidence measurements, and if the intensity of the beam happened to be double during the background run, twice as many accidentals would be recorded per unit beam current as should be recorded. However, it was sometimes apparent that when the intensity was lower than usual, sparks were occurring in the tank, cutting out entire f-m bursts. In this case, the accidental rate was proportional to the beam intensity. As a further check, for one angle of scattering ( $45^\circ$ ), the polyethylene scatterer was replaced by a carbon scatterer seven mils thick. The coincidence counts observed in this case were only one percent of the

-12-

coincidence counts obtained for the same activity of the carbon but with a polyethylene scatterer and were approximately equal to the accidental counts determined by the delayed coincidence rate.

In addition to the background just discussed, both probes continued counting at a reduced rate when the oscillator was turned off. This effect was due to the intense radioactivity present in the cyclotron tank. Theoretically one can discriminate by pulse height against the pulses from electrons, but the gains were set sufficiently high to be sure of getting unusually small proton pulses and hence some electrons were counted. Since these counts were not bunched in time, in contrast to the cyclotron beam, they did not contribute appreciably to the accidental coincidence rate.

#### C. Beam Current Monitoring.

When carbon is bombarded by high energy protons, the only activity formed to any extent is the 20.5 minute positron decay of  $C^{11}$ . In order, therefore to measure the beam current it is necessary to know the ratio of the number of activated  $C^{11}$  atoms in the foil to the total number of atoms, and also to know the cross section for the formation of  $C^{11}$  by the (p,pn) reaction. However, the proton-proton scattering cross section is obtained in terms of the  $C^{11}$  cross section without going through the intermediate process of finding the actual beam current. The total number of atoms in the foil need not be known, but only the ratio of carbon to hydrogen.

In order to find the total number of activated carbon atoms, the target is removed and the  $C^{11}$  activity counted by a thin end window,

-13-

1.5 mg/cm<sup>2</sup>, G-M counter. A close approximation to the number of active carbon atoms that would have been present had none decayed is then obtained by extrapolating the activity back to half bombardment time and dividing by the decay constant  $\lambda$ . The error in this procedure is less than one percent for a five-minute bombardment of a 20.5 minute half-life material. Before each run, the plateau level of the G-M counter was checked with a uranium standard. The level was found to fluctuate as much as four percent from one week to the next, even though the slope was only one percent per 100 volts. The dead time of the counter was measured to be 110  $\mu$  seconds, by counting two samples together and separately assuming  $n_{\text{true}} = n_{\text{obs}}(1 + n_{\text{obs}}\tau)$ . The final data for the 105 Mev points were all taken with the same counter.

To find the order of magnitude of the proton-proton scattering cross section, a rough calibration of the G-M counter efficiency was made. The best way to evaluate the effective solid angle, self-absorption, backscattering and other factors is to measure a known source. It is necessary to use a source with the same properties as the one for which the G-M counter is to be calibrated. To do this, the absolute activity of C<sup>11</sup> in polyethylene foil was measured with scintillation counters, using the method of  $\beta$ - $\gamma$  coincidence counting. In this method the efficiencies of the scintillation counters do not enter the final expression for the absolute activity.

Thus,

$$\text{The number of } \beta \text{ counts } N_{\beta} = N_0 \epsilon_{\beta},$$

$$\text{The number of } \gamma \text{ counts } N_{\gamma} = N_0 \epsilon_{\gamma}.$$



-14-

The number of coincidences  $N_{\beta\gamma} = N_0 \epsilon_{\beta} \epsilon_{\gamma}$ ,

$$\text{giving } N_0 = \frac{N_{\beta} N_{\gamma}}{N_{\beta\gamma}}$$

where  $\epsilon_{\beta}$  and  $\epsilon_{\gamma}$  are the overall efficiencies for counting  $\beta$ 's and  $\gamma$ 's respectively, and  $N_0$  is the absolute activity.  $C^{11}$  decays by emitting a positron, and therefore the source was placed in a small aluminum capsule stopping all the positrons. The annihilation  $\gamma$ -rays all appeared then to come from the same place. A small scintillation crystal was placed in one side of the capsule, which effectively counted only the  $\beta$ -rays, while outside the capsule there was a very large crystal counting the  $\gamma$ -rays. Activity measurements were made alternately with this setup and with the G-M counter. In this way the overall efficiency of the G-M counter was determined to be 1/10.5 for ten-mil polyethylene foils. With five-mil foils the number was 1/9.5 and with 30-mil foils 1/14.3. The fact that the ratio 9.5 to 10.5 was correct was verified by counting two five-mil foils first on top of one another and then alongside. The ratio measured in this way checked the previous ratio to better than one percent, but the absolute efficiency may be incorrect by twenty percent, due to systematic errors.

Care was taken to eliminate certain errors, in the following manner. The amplifiers and scalars were similar to those used for the scattering experiment. In this situation, however, it was necessary that all pulses being counted as single channel counts should also trigger the coincidence circuit, if a true coincidence had occurred. Over a very small range, one volt for the discriminators used here, the output

-15-

pulses were smaller than standard size and would not trigger the coincidence circuit. In order to eliminate this effect the pulses were fed into a second discriminator in series with the first and then directly to a scaler and simultaneously to the coincidence circuit. This arrangement reduced the losses to less than one percent even when counting phototube noise that was barely firing the first discriminator.

#### D. Dee Flaps and Clipper.

When the cyclotron was running at full intensity the average beam current was somewhat more than  $0.1 \mu$  ampere. Since the scattering experiment needed a current of only  $10^{-11}$  ampere or less, three things were done to cut down the beam. First, the ion source filament and hydrogen supply were cut off. Actually, in the final arrangement, the source was left on but helium was used instead of hydrogen to maintain the arc, as will be explained in the next section. Second, adjustable flaps that extended out about fifteen inches from the tank center were installed on the dummy dee. They reduced the dee gap to about  $1/4$  inch. Since the beam oscillates vertically about the central plane, it was necessary to use only one flap to control the intensity. Third, a  $1/4$  inch beam height clipper placed part way around the tank from the target cut down the intensity and in particular increased appreciably the coincidence to single channel rate. The clipper performed another important function in that it cut down the possibility that the beam would make multiple traversals of the target. A calculation of the multiple scattering showed that the protons would hit the clipper after one or two traversals of the target.

### E. Beam Energy

When a cyclotron is operated with the ion source shut off, protons may be formed anywhere within the vacuum tank. As a result, protons may reach the target that started quite far off center. Since the magnetic field tapers off with increasing radius, the orbit of such a proton precesses rapidly. Hence no matter where the proton originates, if it starts off center it arrives at the target early, and with too low an energy. This difficulty manifested itself in many ways in this experiment. First, the burst as viewed on a scope triggered by an f-m receiver arrived too early in the f-m cycle. Second, the plateau positions did not agree with those previously calculated, indicating the low energy particles were striking the target and being bent too far in the magnetic field before reaching the crystals.

To cure the trouble, helium was used to sustain the arc. The beam intensity was now somewhat higher than it was with no ion source. It was then possible to adjust the flaps again so that the intensity of particles that came from places other than the ion source was only ten percent of that due to the source. In this way most of the particles were caused to come from the correct place and at the correct time. When the ion source was thus used, it was still possible to make the protons reach the target too early by firing the arc late. In fact, if the arc was fired 100  $\mu$  seconds after the optimum acceptance time, the burst would appear 250  $\mu$  seconds early. The total acceleration time was 1600  $\mu$  seconds. Similar results have been obtained at Berkeley<sup>12</sup> but

---

<sup>12</sup> Henrich, Sewell, and Vale, Rev. Sci. Inst. 20, 887 (1949).

-17-

of much smaller time magnitude. These investigators explained the phenomenon on the basis of phase oscillations. Particles that started late and out of phase oscillate about the synchronous orbit and may arrive at the target ahead in phase. This type of oscillation does not change the energy with which a particle arrives at the target whereas radial oscillations do.

A separate experiment has been performed by N. Bloembergen and P. van Heerden<sup>13</sup> to determine the energy distribution at 35 inches with the cyclotron in operation for proton-proton scattering as explained above. A half width of seven Mev and a mean energy of 75 Mev was observed. The energy calculated from the magnetic field and radius at the target was 85 Mev. The half width at 40 inches was 8.5 Mev with a mean energy of 105 Mev. No importance is to be attributed to the difference between the half-widths since the measurement at 105 Mev was observed under different operating conditions.

#### F. Cross Fire.

The crystals were originally cut about  $1/2$  inch to  $3/4$  inch thick in the direction that the protons traversed, and about  $1/8$  inch by  $1/4$  inch in cross section. Under these conditions it was found that an appreciable number of particles entered the sides of the crystal rather than passing straight through from front to back. As a result the monitor crystal was too small to count all the recoil protons and true plateaus were not obtained. The effect was apparent only for the small

---

<sup>13</sup> N. Bloembergen and P. van Heerden, Private Communication.

-18-

scattering angles where the protons had to traverse a large arc before reaching the defining crystal. To counteract this trouble, the defining crystals were cut down to 1/8 inch thick. Satisfactory pulse heights could still be obtained with this thickness, and the cross fire was eliminated except in the case of extremely small angles. The results given in the last section do not include these small angle points.

#### G. Final Procedure.

The complete procedure for each point was as follows. About one day was spent lining up the monitor counter, running gain curves and rotation curves. Then after the target was withdrawn, a new target was placed in the vacuum lock and pumped on. After the gate to the tank was opened, the cyclotron was warmed up again for a few minutes. Any activity produced on the target while in the lock was too small to be measured. During this time the standard source was being counted in the G-M counter. Then the new target was let in. It was now necessary to start the counters, turn on the oscillator, run five minutes, turn off the oscillator and turn off the counters. Special care was taken to get the dee volts up rapidly without breakdown and resultant loss in intensity, since the extrapolation procedure in counting the target foils assumed a uniform bombardment. The target was then withdrawn and the activity counted for two three-minute intervals. For each angle two and sometimes four foils were successively bombarded.

#### IV Results and Conclusions

Table I gives typical data obtained for the  $\phi = 45^\circ$  point. An explanation of the headings is as follows. Time of count refers to the

-19-

interval from the start of the bombardment to the center of the three minute interval during which the target activity was counted. The corrected counting rate has had the G-M counter background subtracted and the dead time losses allowed for. The following procedure is employed to obtain  $N_0$ , the total number of  $C^{11}$  atoms formed during the bombardment. The two determinations of the activity are extrapolated back to half-bombardment time and averaged, divided by  $\lambda$ , the decay constant, multiplied by the appropriate geometrical factor for the G-M counter (which depends on the foil thickness used), and normalized to the standard G-M plateau level. The true number of proton-proton coincidences,  $N_{pp}$ , is the difference between the number of counts in the prompt coincidence channel and in the delayed coincidence channel. The differential cross section in the laboratory system is then given by,

$$\frac{d\sigma}{d\Omega} = \frac{N_{pp} \cdot \sigma_c''}{2N_0 \cdot \Delta \Omega}$$

The factor two in the denominator arises from the fact that there are two hydrogen atoms for each carbon atom in polyethylene.

Seventy millibarns at 105 Mev and 81 millibarns at 75 Mev<sup>14</sup> were used for the cross section of the formation of  $C^{11}$  to establish an absolute basis for the value of  $\frac{d\sigma}{d\Omega}$ . The differential scattering cross section in the center of mass system,  $\frac{d\sigma}{d\omega}$ , plotted in Figure 6,

<sup>14</sup> W. W. Chupp and E. M. McMillan, Phys. Rev. 72, 873 (1947) ;  
E. M. McMillan and R. D. Miller, Phys. Rev. 73, 80 (1948) ;  
Aamodt, Peterson, and Phillips, Phys. Rev. 78, 87A (1950) and UCRL-526.

-20-

was obtained from the laboratory cross sections by multiplying by

$$\frac{\sin \bar{\Phi} d\bar{\Phi}}{\sin \phi d\phi} = \frac{1}{4 \cos \bar{\Phi}} \frac{(1 - \beta^2 \cos^2 \bar{\Phi})^2}{1 - \beta^2}$$

which is the relativistic transformation of solid angles. Capital letters indicate the laboratory system, small letters the center of mass system.\*\* The center of mass angles are related to the laboratory angles by the relation

$$\tan \bar{\Phi} = (1 - \beta^2)^{1/2} \tan \phi/2$$

The cross section for each angle is the result obtained by statistically weighting the individual runs at that angle. The values are given with their standard deviations in Table 2. In all runs at a given value of  $\bar{\Phi}$  the same defining solid angle was used for the final data. It was therefore merely necessary to add up the coincidence protons that resulted from all the runs and to divide by the total number of  $C^{11}$  atoms formed. The percent error in the measurement of the carbon activity was small compared to the error in the number of coincidence protons and it will be neglected. The resultant standard deviation in the ratio is then just the square root of the total proton counts, divided by the total activity.

The differential scattering cross section in the center of mass system,  $\frac{d\sigma}{d\omega}$  appears to be constant within the statistical deviation over the range of angles measured. The absolute magnitude of the 105 Mev cross section, 5.6 millibarns, differs somewhat from the value of

---

\*\* The symbols follow the convention established by Hadley, et al.

Phys. Rev. 75, 351 (1949), in their n-p scattering experiment.

-21-

four millibarns obtained recently at Berkeley for 120 Mev protons.<sup>3</sup> As was mentioned earlier, this difference may be due to the calibration procedure for the G-M counter and also to the uncertainty in the cross section for the formation of  $C^{11}$ . The absolute cross section may be in error by as much as 20 percent while the relative differential cross sections should be good to better than 10 percent. It is hoped that experiments now under way at Harvard will determine the carbon cross section more accurately and hence simultaneously the proton-proton cross section. Preparations are also now being made at Harvard for proton-proton scattering experiments with an external beam. These experiments should ultimately be of much higher precision, particularly on absolute cross section, than those so far reported.



-22-

TABLE I

Typical Data For  $\Phi = 45^\circ$ .

Solid angle of defining counter  $\Delta\Omega = 6.70 \times 10^{-4}$   
 Correction to solid angle  $\Psi / \sin\Psi = 1.013$   
 Dead time of G-M counter  $\tau = 110 \mu$  seconds  
 Relativity correction to  $1/4 \cos\Phi = 1.000$

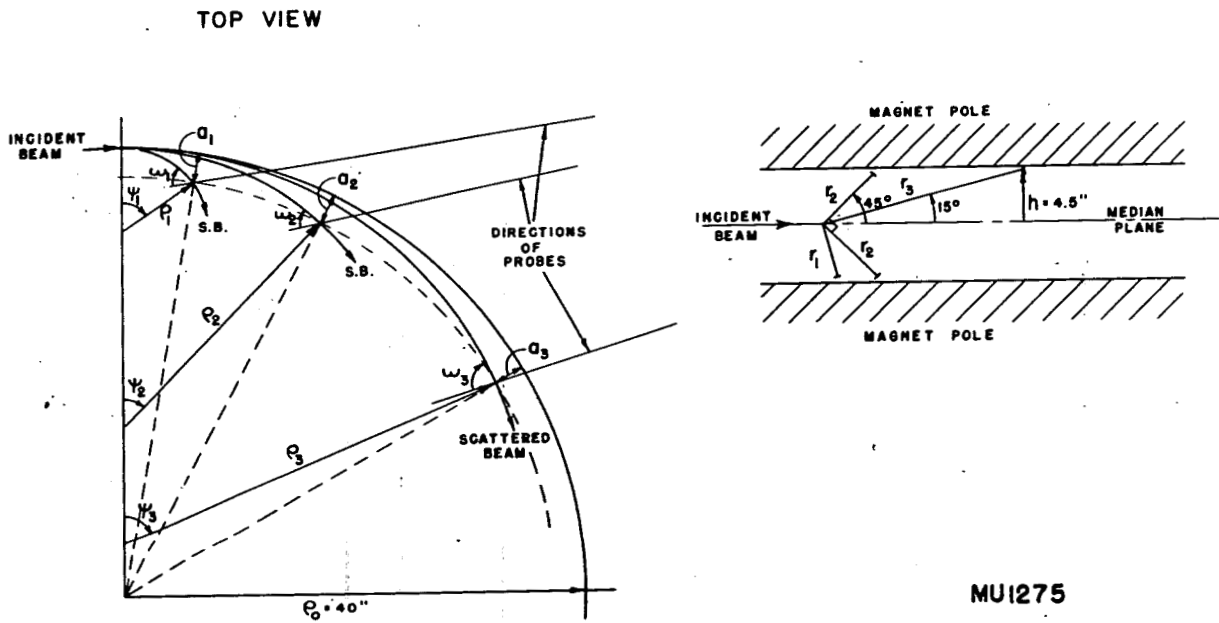
Run no.	Time of count	Corrected Rate 3 minutes x 64	Foil Thickness	$N_{64}$	Coincidence Counts	Background	$N_{pp}$	$\frac{d\sigma}{d\Omega}$ (c")
1a	11.0	207	10 mils	28400	545	10	535	0.216
1b	14.5	182						
2a	11.0	198	5 mils	24500	495	6	489	0.229
2b	14.5	173						
3a	10.5	220	5 mils	26600	547	5	542	0.234
3b	14.0	189						
4a	11.0	354	10 mils	48200	949	17	932	0.222
4b	14.5	305						

TABLE II  
Data plotted in Figure 6

$\Phi$	20°	25°	30°	35°	40°	45°
105 Mev						
$\phi$	41° 8'	51° 19'	61° 30'	71° 41'	81° 42'	91° 42'
$\frac{d\sigma(\phi)}{d\omega}$	5.64 $\pm$ 0.15	5.44 $\pm$ 0.13	5.64 $\pm$ 0.12	5.78 $\pm$ 0.19	5.50 $\pm$ 0.12	5.62 $\pm$ 0.11
75 Mev						
$\phi$	40° 48'	50° 50'	60° 56'	71° 8'	81° 8'	91° 8'
$\frac{d\sigma(\phi)}{d\omega}$	6.12 $\pm$ 0.15	6.61 $\pm$ 0.11	6.45 $\pm$ 0.11	6.35 $\pm$ 0.18	6.78 $\pm$ 0.13	6.48 $\pm$ 0.11

## FIGURE CAPTIONS

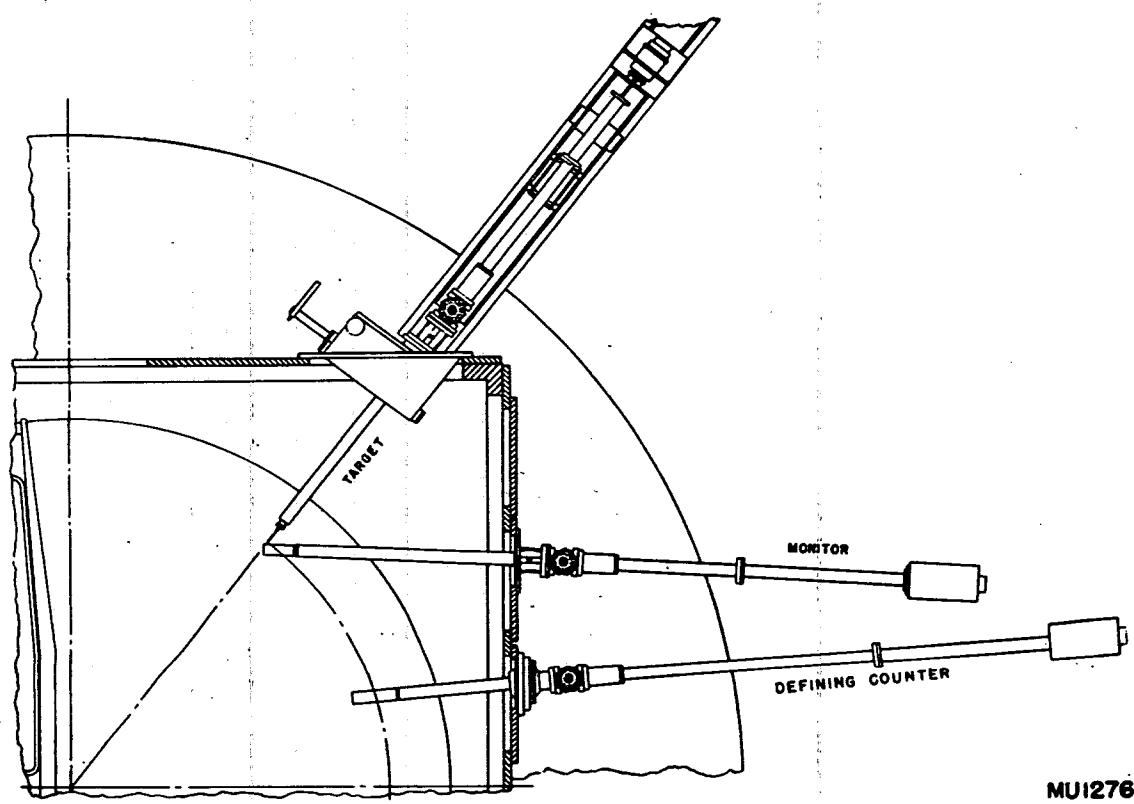
- FIG. 1 Side view showing scattering geometry. Paths drawn as straight lines are actually sections of helices.
- FIG. 2 Plan view of cyclotron tank showing target, monitor, and defining counter probes.
- FIG. 3 Photograph of experimental setup. The vacuum cap has been removed from the monitor probe showing the anthracene crystal. The upper probe is the defining counter and the ball and socket joint through which it passes may be seen mounted in the tank wall.
- FIG. 4 Plot of coincidence rate versus monitor position normalized to the single channel rate in the defining counter. The plateaus in these curves indicate that all the protons are being counted.
- FIG. 5 Plot of coincidence rate versus monitor amplifier gain normalized to the single channel rate in the defining counter. The monitor single channel rate is also shown for comparison but on a scale smaller by a factor of 50.
- FIG. 6 Proton-proton differential scattering cross sections at 105 Mev ( $\frac{1}{2}$ ) and at 75 Mev ( $\frac{1}{4}$ ) versus scattering angle in the center-of-mass system. Absolute values based on the  $C^{12}$  (p,pn)  $C^{11}$  cross section equal to 70 and 81 mb respectively. The standard deviations shown are due only to the statistical fluctuations in the number of protons counted.



MUI275

Fig. 1

26



MUI276

Fig. 2

27

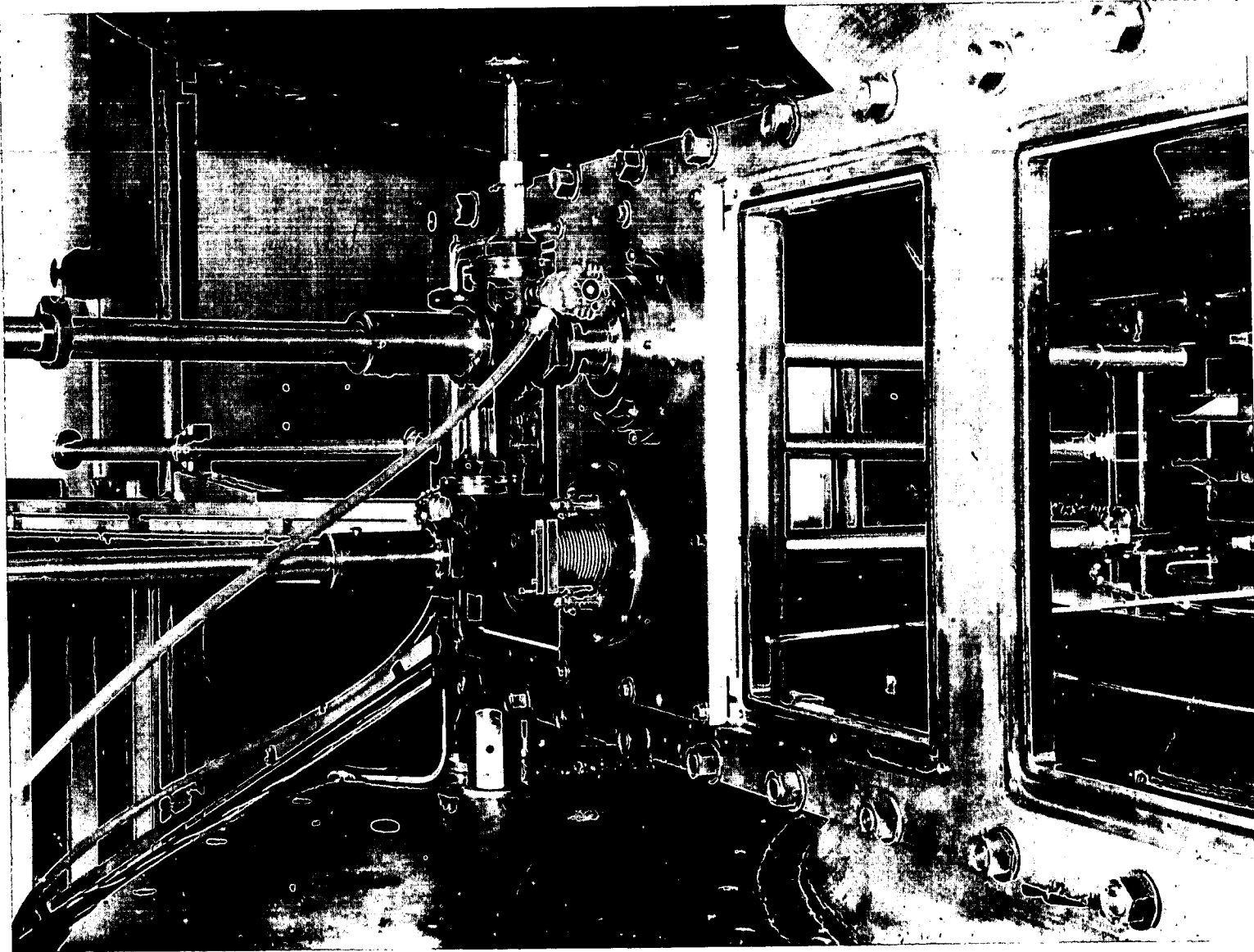


FIG. 3

OZ 1092

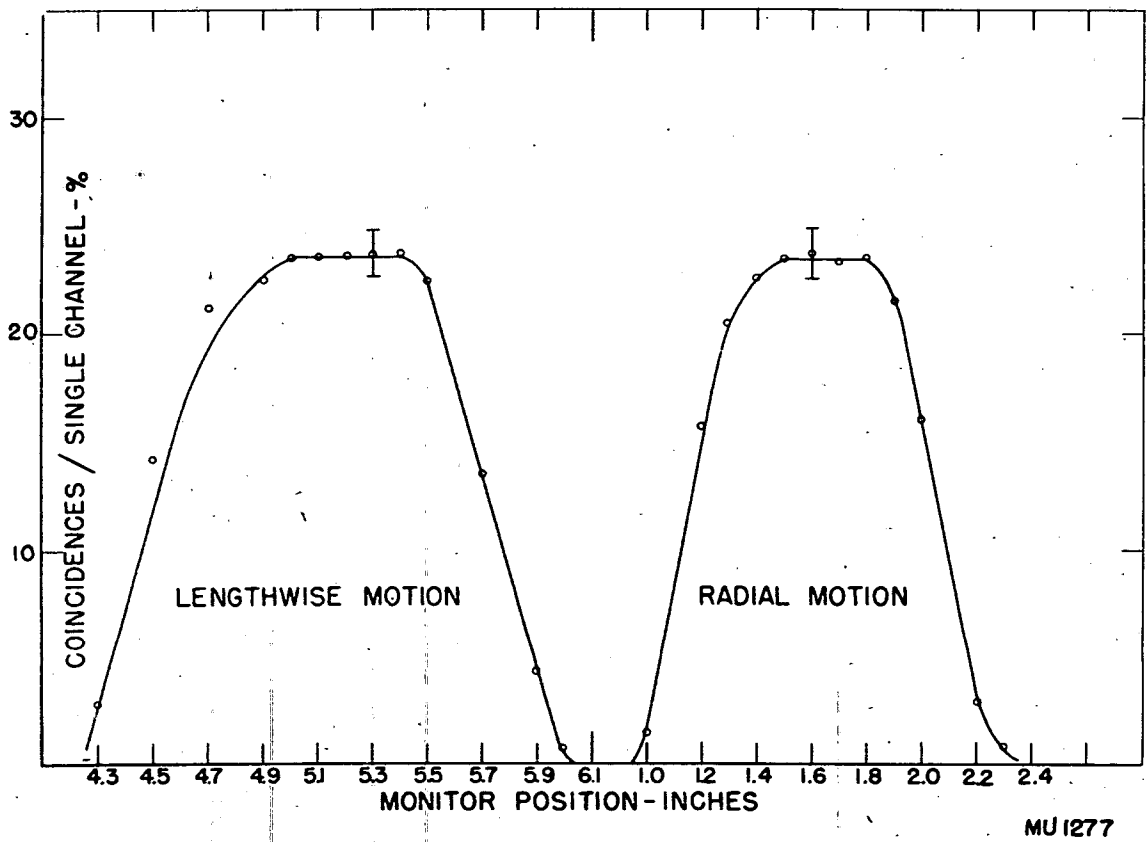


Fig. 4

29

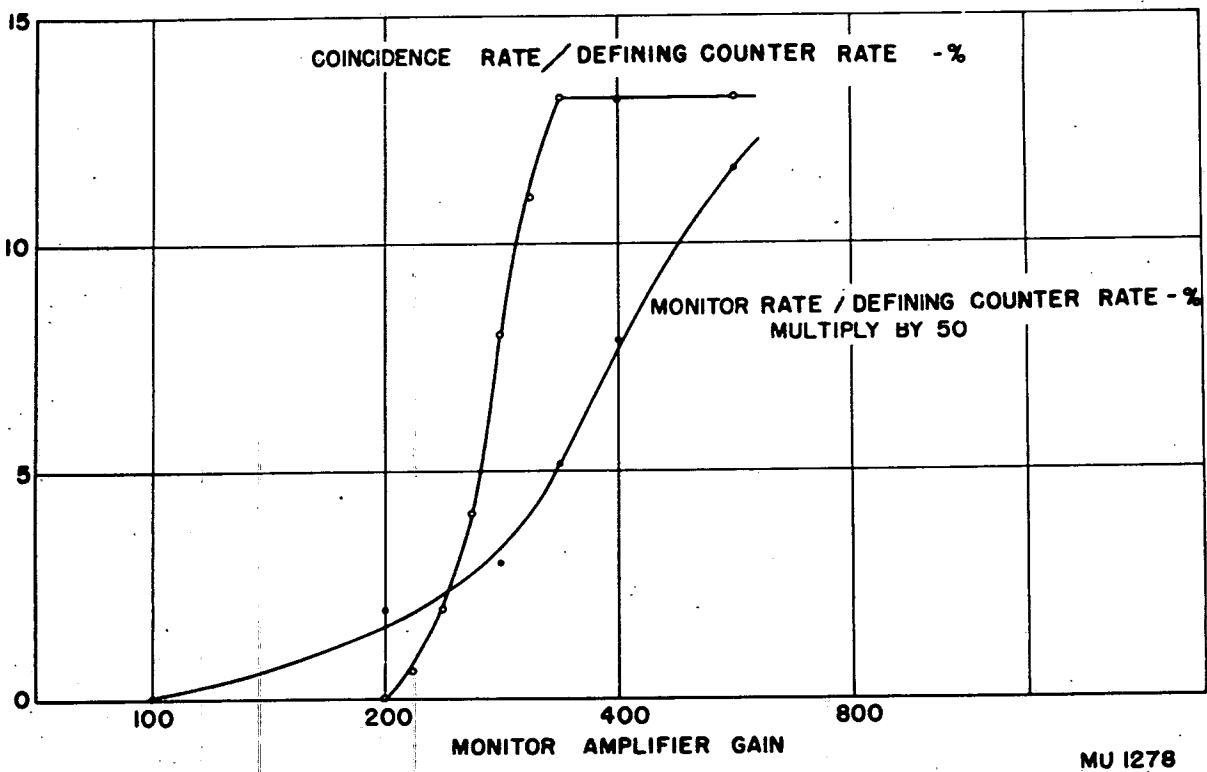
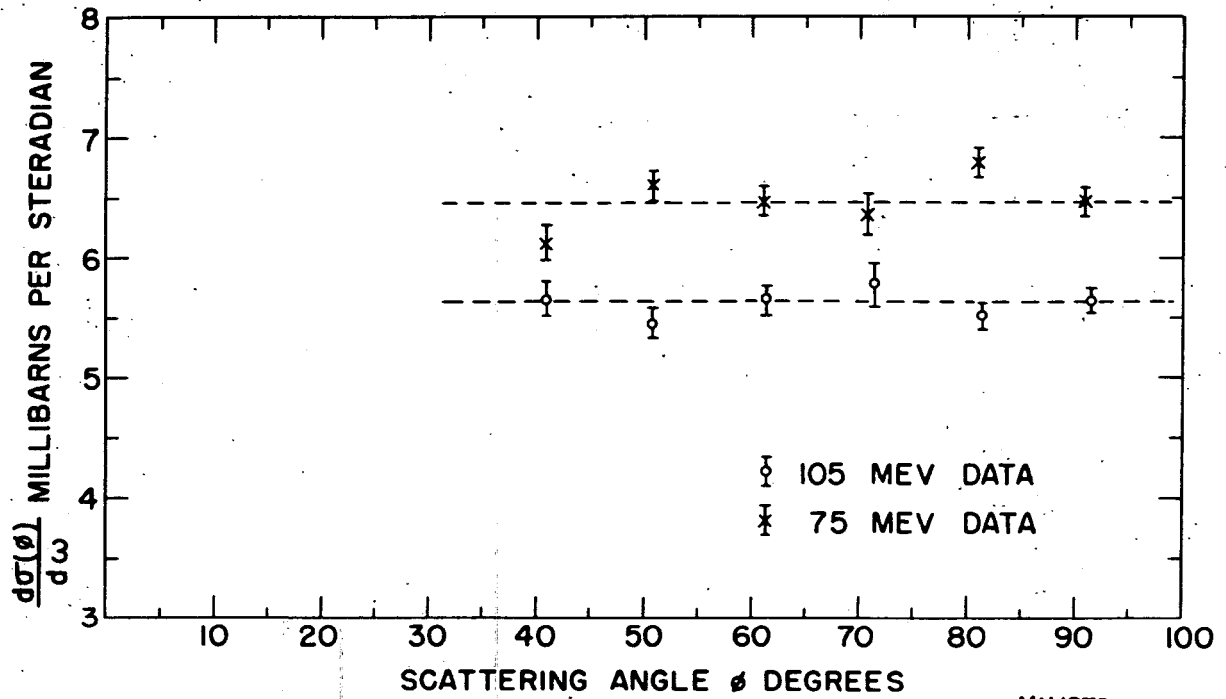


Fig. 5

MU 1278



30



MU1279

Fig. 6